Journal of Modern Physics, 2011, 2, 154-157
doi:10.4236/jmp.2011.23023 Published Online March 2011 (http://www.SciRP.org/journal/jmp)

Magnetic, Structural and Morphological Characterization of Sr_2GdRuO_6 Double Perovskite

L. T. Corredor[1], D. A. Landínez Téllez[1], J. L. Pimentel Jr[2], P. Pureur[2], J. Roa-Rojas[1]
[1]*Grupo de Física de Nuevos Materiales*, *Departamento de Física*, *Universidad Nacional de Colombia, Bogotá DC,Colombia*
[2]*Instituto de Física*, *Universidade Federal do Rio Grande do Sul*, *Porto Alegre, Brasil*
E-mail: *jroar@unal.edu.co.*
Received October 6, 2010; *revised December* 8, 2010; *accepted December* 15, 2010

Abstract

We report structural, morphological and magnetic properties of the Sr_2GdRuO_6 compound, which is used as precursor oxide in the production process of $RuSr_2GdCu_2O_8$ superconducting ruthenocuprates. The crystalline structure was studied by X-ray diffraction and Rietveld refinement. Results reveal that material crystallizes in a monoclinic double perovskite, space group $P2_1/n$ (#14). Scanning Electron Microscopy experiments on samples show homogeneous granular morphology with grain size from 3 up to 7 μm. Semiquantitative analysis of composition was performed by the Energy Dispersive X-ray technique. Experimental results are 98% in agreement with the theoretical stoichiometry. Curves of magnetization as a function of temperature exhibit an antiferromagnetic-like behaviour, with Néel temperature T_N=15.3 *K* and magnetic effective moment 8.72 μ_B.

Keywords: Complex Perovskite, Structure, Magnetic Properties

1. Introduction

The $RuSr_2GdCu_2O_8$ ruthenocuprate oxide was synthesized for the first time in 1995 [1]. It belongs to the $RuSr_2RECu_2O_8$ (Ru-1212RE) family, where RE represents rare earth elements. The main characteristic of these compounds is the presence of magnetic and superconductor properties in a simultaneous way, with magnetic transition temperature higher than the superconductor critical temperature, which make them unique respect to the other magnetic superconductors. Initially, ruthenocuprates were obtained by the solid state reaction with CuO and Sr_2RERuO_6 as precursor oxides [2-4]. The superconductor properties are determined by the Cu-O bonds in the CuO_2 conduction planes, which give rise to critical temperature values between 15 and 50 K [5]. Magnetic properties are associated with Ru-O bonds (RuO_2), even when actually there is no consensus about the magnetic ordering between Ru atoms [6]. Muon Spin Rotation measurements (μSR) point a ferromagnetic ordering normal to *c* crystallographic axis [7], while neutron diffraction experiments indicate an antiferromagnetic response [8]. The main obstacle to define the nature of the superconductor-magnetic mechanisms in this kind of materials is the lack of high purity samples. In order to enhance the knowledge about the synthesis method of $RuSr_2GdCu_2O_8$, we report the high quality production process, a carefully structural Rietveld analysis of X-ray diffraction data, morphologic and compositional studies of the Sr_2GdRuO_6 material. Measurements of magnetic susceptibility as a function of temperature were also performed to observe the possible effects of this precursor material on the magnetic characteristics of the $RuSr_2GdCu_2O_8$ superconductor.

2. Experimental

The Sr_2GdRuO_6 ceramic was obtained by the standard solid state reaction method, from stoichiometric quantities of $SrCO_3$ (Chemi 99.7%), Gd_2O_3 (Aldrich 99.9%) and RuO_2 (Aldrich 99.9%). In order to extract possible humidity, the oxide powders were heated to 200°C for 24h. Then they were weighted, grounded in an agatha mortar, and pressed to form pellets of 9.8 ± 0.1 mm diameter and 1.0 ± 0.1 mm thickness. These pellets were calcined at 930°C for 12 h, cooled up to ambient temperature, regrounded and twice heated in a sinterization process at 1230°C for 16 h. Structural characterization

was performed by the X ray diffraction technique (XRD) through a Panalytical Xpert Pro diffractometer with CuK_α = 1,5406 Å radiation. The morphological characterization was carried out by using a FEI Quanta 200 Scanning Electron Microscope SEM, and the semiquantitative analysis of composition was performed by means Energy Dispersive X-ray (EDX) experiments, with an EDAX microanalysis accessory for the SEM. Magnetization and susceptibility versus temperature measurements were performed through a Quantum Design 2000 MPMS SQUID. Rietveld refinement of experimental XRD data was performed by using the GSAS code [9]. Refinement results were compared with characteristic values predicted by the Structure Prediction Diagnostic Software (SPuDs), which was created for perovskite-like materials [10].

3. Results and Discussion

Figure 1 shows the powder x-ray diffraction pattern for Sr_2GdRuO_6 material. Rietveld refinement of these experimental data is shown too. The continuous curve corresponds to the pattern calculated for Sr_2GdRuO_6 and the symbols represent the experimental diffractogram. In the same graph, locations of Bragg peaks are shown as vertical lines. Curve in bottom of **Figure 1** represents the difference between experimental pattern and the calculated one. From Rietveld refinement we determined that this diffraction pattern is characteristic of a monoclinic perovskite structure, space group $P2_1/n$ (#14).

The discrepancy factor of refinement was χ^2 = 1.063. The final cell parameters found were a = 5.8019(0) Å, B = 5.8296(5) Å, c = 8.2223(7) Å, and Tilt Angle β = 90.258°. The atomic coordinates and relative occupancy of each site are shown in **Table 1.**

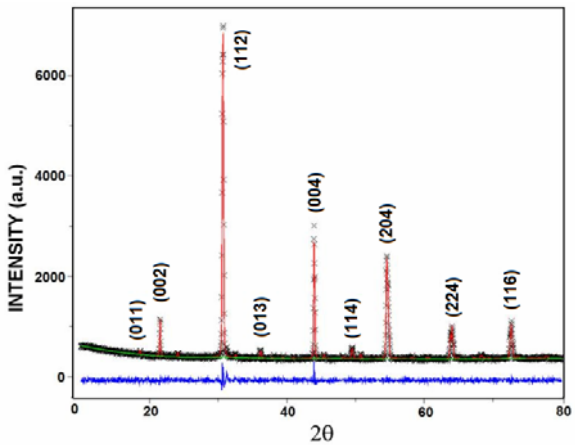

Figure 1. XRD pattern for Sr_2GdRuO_6 complex perovskite. Symbols correspond to the experimental data and continuous one is the obtained by Rietveld refinement. Bottom curve represents the difference between experimental and calculated patterns.

Results are 99 % in agreement with the SPuDs [10], which predicts $P2_1/n$ (#14) space group as very probable. The SPuDs program also predicts the lattice parameters *a* = 5.7537 Å, *b* = 5.9634 Å, *c* = 8.2760 Å, tolerance factor 0.9170 and tilt angle β = 89.9546°. The presence of the (002), (114) and (116) peaks in the diffractogram of **Figure 1** confirms the existence of the superstructure that characterizes the $A_2BB'O_6$ complex perovskites [11].

The values for the bond distances of cations (relative to the oxygen anion) and occupancy were obtained from the Rietveld refinement. These are shown in **Table 2**.

In this double perovskite the explanation of distortion from the ideal cubic perovskite structure is clear because the Sr_2GdRuO_6 complex perovskite have the generic formula $A_2BB'O_6$, and for this type of material the tolerance factor *t*, is calculated by the ratio:

$$\tau = \frac{r_A + r_0}{\sqrt{2}\left(\frac{r_B + r_{B'}}{2} + r_0\right)}$$

where r_A, $r_{M'}$, $r_{M''}$ and r_o are the ionic radii of the A, B, B', and O ions, respectively. If *t* is equal to unity, there is ideal cubic perovskite structure, and if $t < 1$ the structures is distorted from the cubic symmetry, and in agreement to the SPuDs prediction [10], the value of tolerance factor by Sr_2GdRuO_6 complex perovskite is 0.9170. The distortion from the ideal cubic perovskite structure is a consequence of the inclination of the Gd-$O_{6/2}$ and Ru-$O_{6/2}$ octahedra; in the mean time support their corner connectivity. Then, the Ru^{5+} and Gd^{3+} cations occupy two crystallographic independent octahedral sites, namely *2d* and *2c* [12]. Our crystallographic results are in accordance with other reports, but there is no an enhanced characterization about atomic positions and the inter-atomic distances [13].

The alternating distribution between Ru^{+5} and Gd^{+3}, ions on the six coordinate B sites of the double perovskite is in agreement with the results obtained from the refinement of experimental diffraction pattern. On the other hand, the Sr^{2+} is located in the A crystallographicsite, as shown the **Figure 2**.

The surface morphology of Sr_2GdRuO_6 samples was

Table 1. Structural parameters of Sr_2GdRuO_6 found by Rietveld analysis of XRD data.

Atom	Site	*x*	*y*	*z*
Sr	4e	0.5054	0.5309	0.2511
Ru	2c	0.0000	0.5000	0.0000
Gd	2d	0.5000	0.0000	0.5000
O	4e	0.2333	0.2084	0.9773
O	4e	0.2675	0.7408	0.9357
O	4e	0.3856	0.9806	0.2281

Table 2. Inter-atomic distance and occupancy calculated through Rietveld refinement of experimental data.

Cation	Anion & Multipl.	Distance (Å)	Occupancy
Ru(2c)	O(4e) × 2	1.9681	1.00
Ru(2c)	O(4e) × 2	1.9666	1.00
Ru(2c)	O(4e) × 2	1.9677	1.00
Gd(2d)	O(4e) × 2	2.2823	1.00
Gd(2d)	O(4e) × 2	2.2805	1.00
Gd(2d)	O(4e) × 2	2.2821	1.00
Sr(4e)	O(4e) × 1	3.6412	1.00
Sr(4e)	O(4e) × 1	2.8741	1.00
Sr(4e)	O(4e) × 1	2.7532	1.00
Sr(4e)	O(4e) × 1	2.5319	1.00
Sr(4e)	O(4e) × 1	2.9295	1.00
Sr(4e)	O(4e) × 1	3.6321	1.00
Sr(4e)	O(4e) × 1	2.5176	1.00
Sr(4e)	O(4e) × 1	3.7147	1.00
Sr(4e)	O(4e) × 1	3.3141	1.00
Sr(4e)	O(4e) × 1	2.4884	1.00
Sr(4e)	O(4e) × 1	3.4116	1.00
Sr(4e)	O(4e) × 1	2.6425	1.00

studied by SEM images as shown in **Figure 3**. Performed analysis reveals the occurrence of granular topology with size grain between 2 up to 7 μm. As observed in microphotography, grains are strongly diffused between them. It is important to notice that sample evidences a single type of grain.

Through semiquantitative EDX analysis, we obtain that composition of material are 98 % in agreement with theoretical values calculated from stoichiometry of Sr_2GdRuO_6 material. Results are shown in **Table 3**.

It is known that the light characteristic of oxygen on the application of X-ray radiation produces a subestimation of its concentration in material when EDX technique is applied to study composition. From structural, morphologic and compositional characterizations we deduced that no other crystallographic phases or impurities are present in the sample.

The magnetic character of material was analyzed from *dc*-susceptibility experiments as a function of temperature. The results are shown in the **Figure 4**, where the magnetic susceptibility reveal an anomaly close to T = 15.3 *K*. This behavior is usually related with the occurrence of a magnetic ordering transition. Fitting of susceptibility with the Curie-Weiss relation $\chi = \chi_0 + C/(T + T_N)$ reveals that Sr_2GdRuO_6 behaves as an antiferromagnetic material below a Néel temperature T_N = 15.3 K.

In addition, the Curie-Weiss adjust permitted to determine the temperature independent susceptibility χ_o = 0.0181 emu/mol and the effective magnetic moment $P_{eff}\mu_B$ = 8.72 μ_B. Theoretical calculations by the Hund's

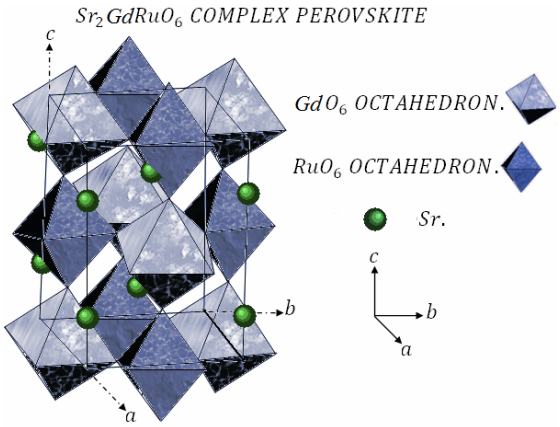

Figure 2. Crystal structure of Sr_2GdRuO_6. The continuous black lines indicate the primitive perovskite unit cell.

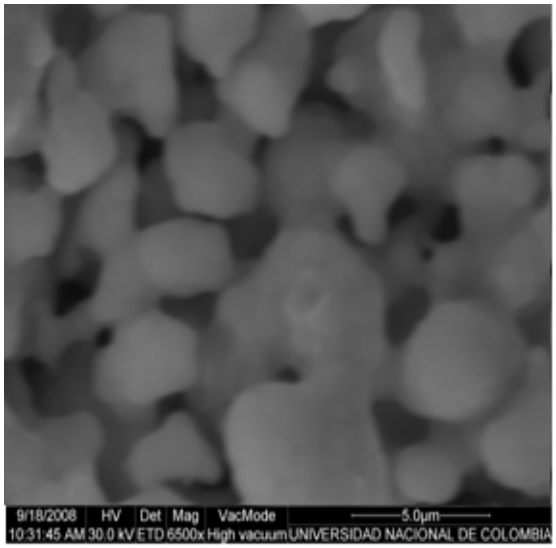

Figure 3. SEM micrograph for Sr_2GdRuO_6 double perovskite obtained from ETD detector (secondary electrons).

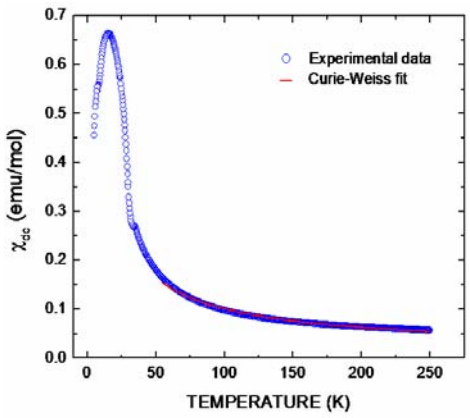

Figure 4. Measurements of dc Susceptibility for Sr_2GdRuO_6 on the application of H = 0.1 T. In picture, circles are the experimental data and the line represents the Curie-Weiss fitting.

Table 3. Results of semi quantitative EDX analysis for the Sr_2GdRuO_6 sample.

Atom	Theoretical %Wt	Experimental %Wt
Sr	33.09	33.82
Ru	29.69	30.05
Gd	19.09	19.78
O	18.03	16.35

rule, with $P_{eff} = g\sqrt{J(J+1)}$, predict that magnetic moments of the isolated ions Gd^{3+} and Ru^{5+} must be $\mu_{Gd}{}^{3+} = 7.94\mu_B$ and $\mu_{Ru}{}^{5+} = 3.87\mu_B$, respectively [14]. The effective magnetic moment of Sr_2GdRuO_6 is obtained to be $\mu_{eff} = 8.83\mu_B$, where we have used $\mu_{eff} = \sqrt{\mu^2_{Gd^{3+}} + \mu^2_{Ru^{5+}}}$ This result corresponds to 98.3% of agreement between experimental and theoretical values. Below T_N, it is observed that the antiferromagnetic ordering becomes to orientate spins anti-parallel to the applied field direction and the magnetic susceptibility decreases.

4. Conclusions

We have performed an experimental study on crystalline structure, surface morphology, composition and magnetic response of Sr_2GdRuO_6 oxide ceramic. Rietveld refinement of X-ray diffraction pattern showed that material crystallizes in a monoclinic complex perovskite structure with space group $P2_1/n$ (#14), with an alternating distribution between Ru^{+5} and Gd^{+3} ions on the six coordinate B sites of the complex perovskite. The presence of the crystallographic peaks (002), (114) and (116) in the diffractogram confirms the existence of the superstructure that characterizes the $A_2BB'O_6$, Complex perovskites. The image of scanning electron microscopy reveals the strongly compact characteristic of grains with sizes from 2 up to 7 μm. The results of Energy Dispersive X-ray experiments show that the composition of the material corresponds in a 98% to the expected stoichiometry of Sr_2GdRuO_6 complex perovskite. Magnetic susceptibility experiments permitted to determine the occurrence of a paramagnetic-antiferromagnetic transition with a Néel temperature of 15.3 K. From the analysis of susceptibility curves we found the effective magnetic moment to be $8.72\mu_B$. In the dc susceptibility curve it is possible to observe a tendency to the antiferromagnetic ordering below the Néel temperature.

5. Acknowledgements

This work was partially supported by the Colombian agencies Colciencias, the Division of Investigations, Universidad Nacional de Colombia (DIB - Bogotá), and Brazilian CNPq.

6. References

[1] L. Bauerfeind, W. Widder and H. F. Braun, *Physica C*, Vol. 254, 1995, p. 151. doi:10.1016/0921-4534(95)00574-9

[2] T. P. Papageorgiou, T. Herrmannsdörfer, R. Dinnerbier, T. Mai, T. Ernst, M. Wunschel and H. F. Braun, *Physica C* , Vol. 377, 2002, p. 383. doi:10.1016/S0921-4534(01)01291-6

[3] L. T. Yang, J. K. Liang, Q. L. Liu, C. Q. Jin, X. M. Feng, G. B. Song, J. Luo, F S. Liu and G. H. Rao, *Journal of Solid State Chemistry*, Vol. 177, 2004, p. 1072. doi:10.1016/j.jssc.2003.10.015

[4] L. T. Corredor, J. Velasco Zárate, D. A. Landínez Téllez, F. Fajardo, J. Arbey Rodríguez and M. J. Roa-Rojas, *Physica B*, Vol. 404, 2009, p. 2733. doi:10.1016/j.physb.2009.06.078

[5] T. Nachtrab, C. Bernhard, C. T. Lin, D. Koelle and R. Kleiner, *C. R. Physique*, Vol. 7, 2006, p. 6885. doi:10.1016/j.crhy.2005.11.010

[6] A. A. Vasiliev, M. Aindow, Z. H. Han, J. I. Budnik, W. A. Hines, P. W. Klamut, M. Maxwell and B. Dabrowski, *Applied Physic Letters*, Vol. 85, 2004, p. 3217. doi:10.1063/1.1805176

[7] C. Bernhard, J. L. Tallon, C. Niedermayer, T. Blasius, A. Golnik, E. Br¨ucher, R. K. Kremer, D. R. Noakes, C. E. Stronach, and E. J. Ansaldo, *Physical Review B*, Vol. 59, 1999, p. 14099. doi:10.1103/PhysRevB.59.14099

[8] J. D. Jorgensen, O. Chmaissem, H. Shaked, S. Short, P. W. Klamut, B. Dabrowski, J. L. Tallon, *Physical Review B*, Vol. 63, 2003, p. 054440. doi:10.1103/PhysRevB.63.054440

[9] A. C. Larson and R. B Von Dreele, "General Structure Analysis System (GSAS)," *Los Alamos National Laboratory Report LAUR*, 2000, p. 86.

[10] M. W. Lufaso and P. M. Woodward, *Acta Crystallographica B*, Vol. 57, 2001, p. 725. doi:10.1107/S0108768101015282

[11] C. J. Howard, B. J. Kennedy and P. M. Woodward, *Acta Crystallographica B*, Vol. 59, 2003, p. 463. doi:10.1107/S0108768103010073

[12] R. Sáez-Puche, E. Climent-Pascual, R. Ruiz-Bustos, M. A. Alario-Franco and M. T. Fernández-Díaz, *Progress in Solid State Chemistry* Vol. 35, 2007, p. 211. doi:10.1016/j.progsolidstchem.2007.02.001

[13] Y. Doi and Y. Hinatsu, *Journal of Physics Condensed Matter*, Vol. 11, 1999, p. 4813. doi:10.1088/0953-8984/11/25/302

[14] N. W. Ashcroft and N. D. Mermin, *Solid State Physics*, Saunders College Publishing, Fort Worth, 1976, p. 657.

